Current Research in Microbial Sciences 8 (2025) 100380

Contents lists available at ScienceDirect

Current Research in Microbial Sciences

journal homepage: www.sciencedirect.com/journal/current-research-in-microbial-sciences

Linalool exhibit antimicrobial ability against *Elizabethkingia miricola* by disrupting cellular and metabolic functions

Mingwang He [a,1], Weiming Zhong [c,1], Rongsi Dai [a], Su Long [a], Ying Zhou [a], Tongping Zhang [a], Boyang Zhou [a], Tao Tang [a], Linlin Yang [a], Sifan Jiang [a], Wenbin Xiao [b], YanJiao Fu [b], Jiajing Guo [b,*], Zhipeng Gao [a,*]

[a] Fisheries College, Hunan Agricultural University, Changsha 410128, Hunan Province, China
[b] Hunan Agriculture Product Processing Institute, Dongting Laboratory; International Joint Lab on Fruits &Vegetables Processing, Quality and Safety; Hunan Provincial Key Laboratory of Fruits &Vegetables Storage, Processing, Quality and Safety; Hunan Academy of Agricultural Sciences, Changsha 410125, Hunan Province, China
[c] College of Animal Science, Fujian Agriculture and Forestry University, Fuzhou 350002, Fujian Province, China

ARTICLE INFO

Keywords:
E. miricola
Linalool
Antibacterial activity
Transcriptomic analysis
Metabolomic analysis

ABSTRACT

Elizabethkingia miricola is a gram-negative bacillus, a life-threatening pathogen in humans and animals. Linalool, a naturally occurring monoterpene alcohol found in plant volatile oils, exhibits highly effective antibacterial properties. This study investigated the antibacterial activity and mechanism of linalool against *E. miricola*. Initially, linalool showed potent antibacterial activity against *E. miricola*, with inhibition zone (ZOI), MIC, and MBC values of 36.41 ± 1.23 mm, 0.125 % (v/v, 1.0775 mg/mL), and 0.125 % (v/v, 1.0775 mg/mL), respectively. Secondly, it was observed by electron microscopy that linalool caused crumpling, depression, and size reduction of the cells. Linalool affected cell membrane integrity, causing membrane damage and rupture. Thirdly, transcriptome analysis suggested that linalool affected C5-branched-chain dicarboxylic acid metabolism and the biosynthesis of valine, leucine, and isoleucine, result in increased energy production to linalool stress. Linalool disrupted cell division and RNA function in *E. miricola*, and the cells responded to linalool-induced oxidative damage by up-regulating the expression of *msrB* and *katG* genes. Fourthly, metabolome analysis revealed an increase in metabolites related to the glycerophospholipid metabolic pathway and NADP content in *E. miricola*, which may be a metabolic response to linalool stress. Taken together, these findings provide a theoretical basis for the antibacterial mechanism of linalool and suggest potential applications for preventing *E. miricola* infections.

1. Introduction

The genus *Elizabethkingia* are Gram-negative bacteria belonging to the Flavobacteriaceae family, characterized as aerobic, non-motile, non-fermenting, non-spore-forming rods capable of producing indole (Kim et al., 2005; Breurec et al., 2016; Colapietro et al., 2016). In immunocompromised patients and newborns, *Elizabethkingia* spp. are associated with various illnesses including meningitis, keratitis, bacteremia, and pneumonia (Lin et al., 2017; Bulagonda et al., 2018; Peng et al., 2020). The genus *Elizabethkingia* currently includes seven distinct species: *E. meningoseptica, E. anophelis, E. miricola, E. bruuniana, E. ursingii, E. occulta*, and *E. argenteiflava* (Doijad et al., 2016; Hwang et al., 2021; Yang et al., 2021). Among these, *E. meningoseptica, E. anophelis*, and *E. miricola* are notable pathogens. *E. meningoseptica*, first reported in 1959 from infants with meningitis, is a significant opportunistic pathogen in humans, rarely infecting immunocompetent adults(King, 1959). In aquaculture, it also causes severe cataract disease in tiger frogs (*Rana tigerina rugulosa*) (Xie et al., 2009). *E. anophelis*, discovered from the Anopheles gambiae intestine in 2011, exhibits resistance to multiple antibiotics, with bacteraemia characterized by high morbidity and mortality rates (Kämpfer et al., 2012; Lau et al., 2016; Shirmast et al., 2021).

E. miricola was isolated from Space Station Mir condensate in 2003 (Li et al., 2003), can cause sepsis (Green et al., 2008), bacteremia (Rossati et al., 2015; Howard et al., 2020; Penven et al., 2020), intracranial infections (Gao et al., 2021), urinary tract infections (Gupta

* Corresponding authors.
E-mail addresses: guojiajing1986@163.com (J. Guo), gaozhipeng627@163.com (Z. Gao).
[1] These authors share first authorship.

https://doi.org/10.1016/j.crmicr.2025.100380

Available online 23 March 2025

et al., 2017; Badawi et al., 2022), and joint infections (Calatrava et al., 2020) in patients. In recent years, *E. miricola* has emerged as a vital pathogen in frog farming, causing septicemia and resulting in substantial economic losses(Hu et al., 2017; Lei et al., 2019; Wei et al., 2023b). Multiregional outbreaks of meningitis-like disease caused by *E. miricola* were confirmed in black-spotted frog (*Pelophylax nigromaculatus*) farms in China in 2016, characterized by symptoms such as sloping neck, cataracts, and high mortality rates (Hu et al., 2017). *E. miricola* can also cause severe infections in the Chinese spiny frogs (*Quasipaa spinosa*), characterized by corneal clouding, ascites, and histopathological damage to organs (Lei et al., 2019). In tiger frog, *E. miricola* is highly pathogenic, causing cataract disease (Xie et al., 2009). Furthermore, *E. miricola* infection in bullfrog (*Lithobates catesbeiana*) have been reported to caused high pathogenicity and mortality in many American bullfrog farms (Wei et al., 2023b). The intensification and high-density practices of frog farming have made frogs increasingly susceptible to infectious diseases, particularly to *E. miricola* induced frog meningitis. This has resulted in substantial economic losses for farmers, posing a significant obstacle to the growth and expansion of frog farming.

E. miricola has been reported to be resistant to a variety of antibiotics, and a study found that *E. miricola* isolated from the brains of five bullfrogs had a high rate of resistance to gentamicin, florfenicol, neomycin, penicillin, amoxicillin, doxycycline, and sulfadimethoxine (Wei et al., 2023a). Similarly, Whole genome sequencing of *E. miricola* revealed 27 putative resistance genes and 38 predicted virulence-associated genes, with 2 novel metallo-β-lactamase genes (*blaBloB-16* and *blaBog-19*) in an isolate from an amphibian (Yang et al., 2023). Furthermore, *E. miricola* possesses a significant number of antibiotic resistance genes, such as *BlaGOB-13* and *BlaB-6* (Opota et al., 2017; Yang et al., 2021). Misuse of antibiotics may lead to ineffective treatment outcomes and promote the emergence of drug-resistant strains, while also contributing to environmental pollution and human health risks. Hence, there's a critical need for alternative, natural therapies with antimicrobial properties to reduce reliance on antibiotics.

Linalool is an acyclic monoterpene alcohol with unsaturated characteristics, commonly contained in volatile oils derived from various aromatic plant species found in nature (Mączka et al., 2022). Linalool is considered safe and has been found to demonstrate antibacterial activity (Abd El-Baky and Hashem, 2016), anti-inflammatory (Kim et al., 2019), anti-cancer effects (Zhao et al., 2020; Elbe et al., 2022), apoptotic and antiproliferative effects (Kisacam et al., 2022). Linalool exhibits antimicrobial activity against a broad spectrum of bacterial species, such as *Pseudomonas aeruginosa* (Liu et al., 2020), *Listeria monocytogenes* (Gao et al., 2019), *Trichophyton rubrum* (Lima et al., 2017), *Shewanella putrefaciens* (Guo et al., 2021a), *Pseudomonas fluorescens* (Guo et al., 2021b), *Pseudomonas fragi* (Li et al., 2022), *Shigella sonnei* (Su et al., 2022), etc. Although the antimicrobial effect of linalool against gram-negative bacteria has been reported in a number of cases, specific studies on *E. miricola* are scarcer. Therefore, there is a critical imperative to investigate the antibacterial efficacy of linalool specifically targeting *E. miricola*.

The aims of the current research were to evaluate the effectiveness of linalool against *E. miricola*, and investigate its potential mechanism of action through microscopic observations, transcriptomic and metabolomic analysis. Furthermore, the purpose of this study was to provide a theoretical basis for the development of linalool as a novel therapeutic agent for treating frog meningitis.

2. Materials and methods

2.1. Materials

Our laboratory isolated and identified *E. miricola* (HZEA 17,093, SUB14992503) from diseased black-spotted frogs that were frozen at −80 °C. *E. miricola* was cultured for 12 h in a 120 rpm shaker at 28 °C using TSB medium. Linalool ((*R*)-(-)-3,7-dimethyl-1,6-octadien-3-ol) solution (95 %) was purchased from Sigma-Aldrich (Sigma-Aldrich, Burlington, MA, USA).

2.2. Agar diffusion assay

Following an overnight incubation period at 28 °C, a bacterial solution (1×10^6 cfu/mL) was applied onto MH (Müller-Hinton agar) plates and evenly distributed. Subsequently, a 6 mm sterile filter paper soaked in linalool was positioned in the middle of each MH plate. The sterile filter paper containing florfenicol was used as a positive control group and the sterile filter paper containing PBS was used as a blank control group. The plates were subsequently subjected to incubation in a constant temperature incubator for a period of 24 h after a 10 min standing time. Measurement of the size of the circle of inhibition produced by the effect of linalool were carried out in triplicate.

2.3. The minimum inhibitory concentration (MIC) and minimum bactericidal concentration (MBC)

The antibacterial effectiveness of linalool was investigated by measuring the observable growth of microorganisms in culture medium using the conventional broth dilution method (CLSI M07-A8) (Parvekar et al., 2020). *E. miricola* was cultured to log phase and then the bacterial concentration in the medium was adjusted to 1×10^6 cfu/mL. Linalool was serially two-fold diluted at concentrations ranging from 8 % (68.96 mg/mL) to 0.015625 % (0.1347 mg/mL). The experimental group was a 96-well plate with equal volumes (100 μL) of drug dilution solution and diluted bacterial solution. Negative controls included the sterile TSB, while positive controls included the diluted bacterial solution and sterile TSB. Following a 24 h incubation at 28 °C, the MIC was determined as the lowest concentration at which no visible bacterial growth was observed in the 96-well plate. The MBC was identified as the minimum concentration that resulted in sterile growth when the bacterial solution from the wells was inoculated onto sterile TSA.

2.4. Antibacterial kinetics

TSB medium with different linalool concentrations (mixed with 1 % Tween 20) was prepared in triplicate, positive controls included the diluted bacterial solution and sterile TSB. The bacterial concentration in the medium was adjusted to 1×10^6 cfu/mL and then incubated in an inverter shaker at 28 °C. OD_{600} absorbance values at 0, 2, 4, 6, 8, 10, 12, 14, 16, 20, 24, 28, 32, 36, 48, 60, 84, 108, 142, 166, 190, 214, 250 h were measured using a spectrophotometer (UV759S).

2.5. XTT reduction assay

Referring to (Xiao et al., 2024a), overnight cultures were centrifuged at 4000 rpm and resuspended in phosphate-buffered saline (PBS; pH 7.2), 0.25 × MIC (0.015625 %), 0.5 × MIC (0.03125 %), and 1 × MIC (0.0625 %) linalool and the concentration of cultures in each tube was adjusted to 1×10^8 cfu/mL, divided into 3 parallel groups. Linalool treatments were carried out at different concentrations for 0.25, 0.5, 1, 1.5, and 2 h, respectively. After treatment, the samples were washed 3 times with sterile PBS and then resuspended. Sodium 3′-[1-(phenylaminocarbonyl)-3,4-tetrazolium]-bis (4-methoxy-6-nitro) benzene sulfonic acid hydrate (XTT, Sigma-Aldrich, MA, USA) labeling reagent and the electroncoupling reagent were mixed in a 50:1 ratio as the XTT meta-naphthoquinone reagent. In a 96-well plate, add 100 μL of resuspension solution and 50 μL of XTT labeling solution (with XTT concentration at 0.3 mg/mL) were added. The absorbance OD_{450} values were measured by a multifunctional enzyme marker after incubation in a water-tight incubator at 28 °C for 4 h. The following formula was used to calculate the survival rate:

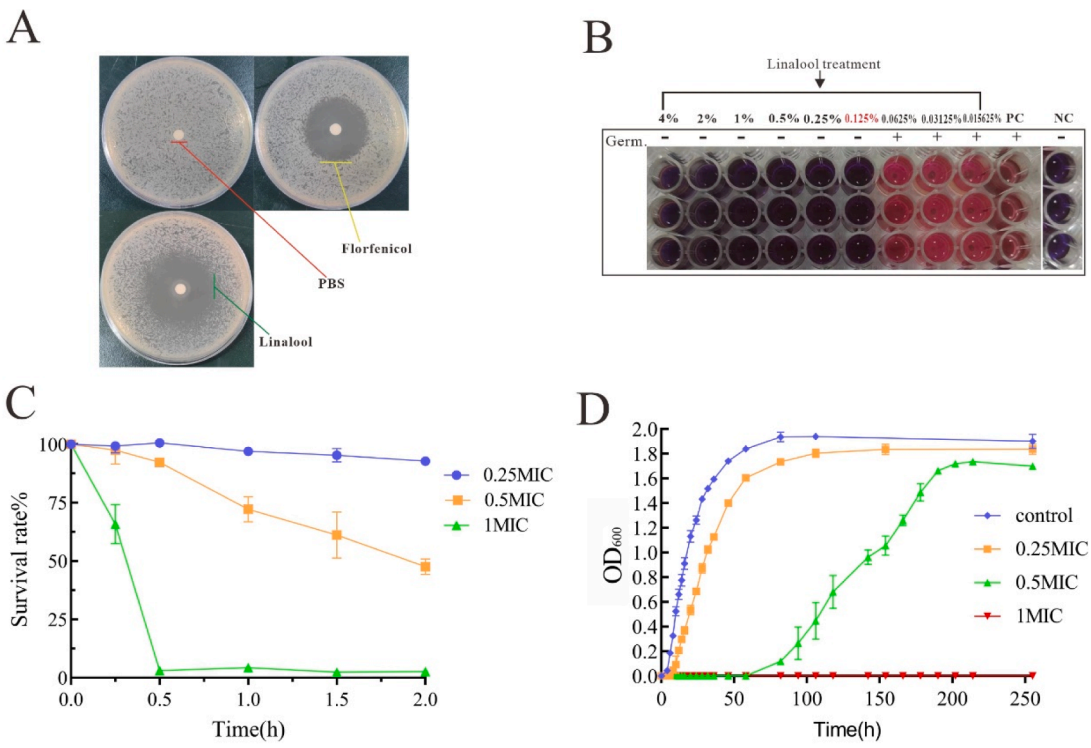

Fig. 1. The antibacterial activity of linalool against *E. miricola*. (A) Zone of inhibition of linalool and florfenicol against *E. miricola*. (B) MIC of linalool against *E. miricola*. NC included the sterile TSB. PC included the diluted bacterial solution and sterile TSB. (C) Bactericidal activity of various concentrations of linalool against *E. miricola*. (D) The antibacterial kinetic curves of linalool against *E. miricola* over time.

$$\text{Survival rate } (\%) = \left(1 - \frac{A_{450}(\text{control}) - A_{450}(\text{treatment})}{A_{450}(\text{control})}\right) \text{x}100\%$$

2.6. Fluorescence microscopy

SYTO 9 Green Fluorescent Nucleic Acid Stain (SYTO 9) is an active cell nucleic acid fluorescent dye (ThermoFisher, USA), producing green fluorescence in living *E. miricola*. If the cell membrane is intact, propidium iodide fluorescent stain (ThermoFisher, USA) cannot enter the cell, and if the bacterial cell membrane is destroyed, propidium iodide fluorescent stain will stain the bacteria with red fluorescence. To prepare the fluorescent staining dilutions, SYTO 9 Fluorescent Dye and Propidium Iodide Fluorescent Dye were diluted with sterile water. After the bacteria were treated with 0.5 × MIC and 1 × MIC linalool for 1 h and washed twice with sterile PBS, the two fluorescent dye dilutions were added separately to the samples and incubated for 20–30 min under light-free conditions. The samples were then washed twice with sterile PBS and resuspended. Add 5 μL of the resuspension dropwise onto a sterile slide and cover with a sterile coverslip. The samples were placed under an inverted fluorescence microscope (OLYMPUS-IX53) for observation.

2.7. Scanning electron microscope

E. miricola was cultured to logarithmic stage and then treated with 1 × MIC linalool for 15, 30, and 60 min, and then washed twice with sterile PBS. Samples were fixed using 2.5 % glutaraldehyde and then washed with sterile PBS to remove the fixative. Samples were dehydrated with a gradient concentration of ethanol; Finally, samples were replaced with tert-butanol, resuspended, and freeze-dried by vacuum in a freeze-drying apparatus (VFD-21S) to remove tert-butanol. The samples were then coated with gold by a magnetron ion sputterer (MSP-2S) and observed by a scanning electron microscopy (Hitachi SU8010).

2.8. Florescent microscope observation

TSB medium was added with low melting point agar, bacteria were stained by SYTO 9 (5 μM) and FM4–64 (40 μmol/l) (ThermoFisher, USA) dyes and mixed with agar medium (Xiao et al., 2024b). The mixtures were aspirated into a glass bottom cell culture dish and placed under a confocal laser scanning microscope (CLSM) (LSM880, Zeiss, Germany). After imaging, a fixed area was selected and linalool solution was added dropwise, imaging was done every 30 min to observe changes in staining of the bacteria in the fixed area.

2.9. RNA-Seq and bioinformatics analysis

E. miricola bacteria were cultured in linalool TSB medium at 0 × MIC and 0.25 × MIC concentrations for 1 h in three parallel groups. Bacterial samples were collected by centrifugation at 4000 rpm with approximately 500 μL per collection. RNA quality was determined by isolating total bacterial RNA and then measuring the OD_{260} nm/OD_{280} nm ratio, with values between 1.8 and 2.0 for all samples. To prepare the library, rRNA was removed from the RNA samples and the mRNA fragments were fragmented into 200 bp fragments. The mRNA fragments were then transcribed into a first strand cDNA and the second strand cDNA was synthesised. the second strand of the cDNA was digested using UNG enzyme to generate the library. After quality control, the sequencing data is filtered and the raw reads are further filtered into clean reads. The clean data (reads) were compared with the reference genome to obtain mapped data (reads) for subsequent analyses. Basic functional annotation was performed on the provided reference genome, and the corresponding functional annotation information was obtained based on the protein sequences compared with six major databases (NR library, swiss-prot library, Pfam library, COG database, GO database, and KEGG database). The expression levels of the genes were quantitatively analysed using the software RSEM, respectively. After obtaining the Read Counts of the genes, the differential expression analysis of the genes

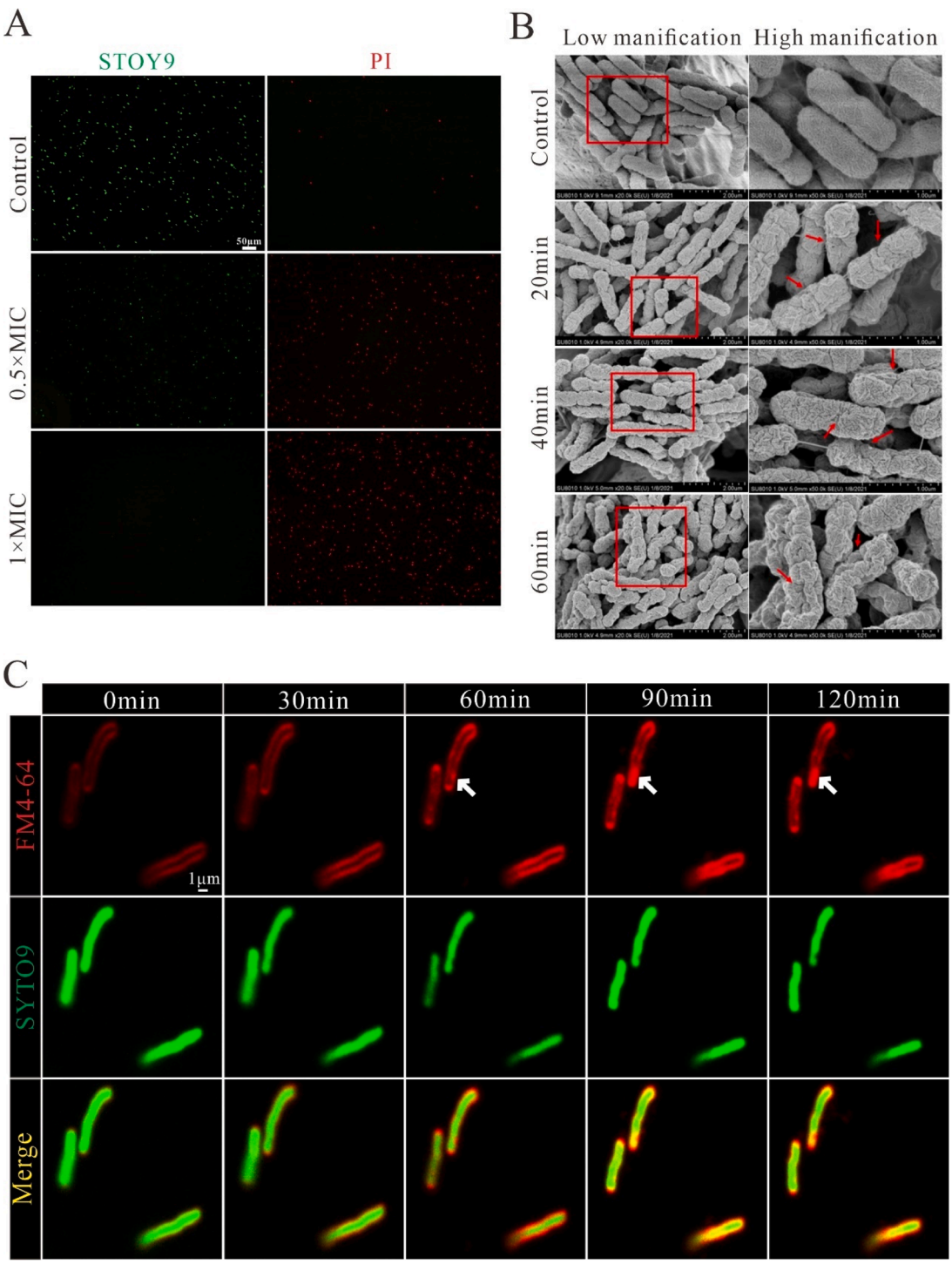

Fig. 2. Effect of linalool on *E. miricola* morphology. (A) The effects of linalool on the viability of *E. miricola* were observed using PI staining assay. Control (without linalool), 0.5 × MIC (0.0625 %) and 1 × MIC (0.125 %) of linalool treatment. (B) SEM images of *E. miricola* treated and untreated with linalool. Untreated bacteria (Control group); 1 × MIC of linalool treated bacteria for 20, 40 and 60 min (Experimental group). The image on the right was an enlarged view of the red rectangle on the left image, with red arrows indicating the folded surfaces of the cells. (C) florescent microscopy images of *E. miricola* treated with linalool for 0, 30, 60, 90, and 120min. White arrows indicated fluorescence penetrating into the cells.

between the samples was performed, and the differentially expressed genes between the samples were identified and the gene sets were established. The differentially expressed genes in the gene set were analysed by GO enrichment using the software Goatools, so as to obtain the main GO functions of the genes in the gene set. The method used was Fisher's exact test, and when the corrected P-value (Padjust) was <0.05, it was considered that there was a significant enrichment of this GO function. KEGG PATHWAY enrichment analysis was performed on the differentially expressed genes in the gene set by using R script, the calculation principle is the same as GO function enrichment analysis, when the corrected P value (Padjust) <0.05, it is considered that there is a significant enrichment of this KEGG PATHWAY function.

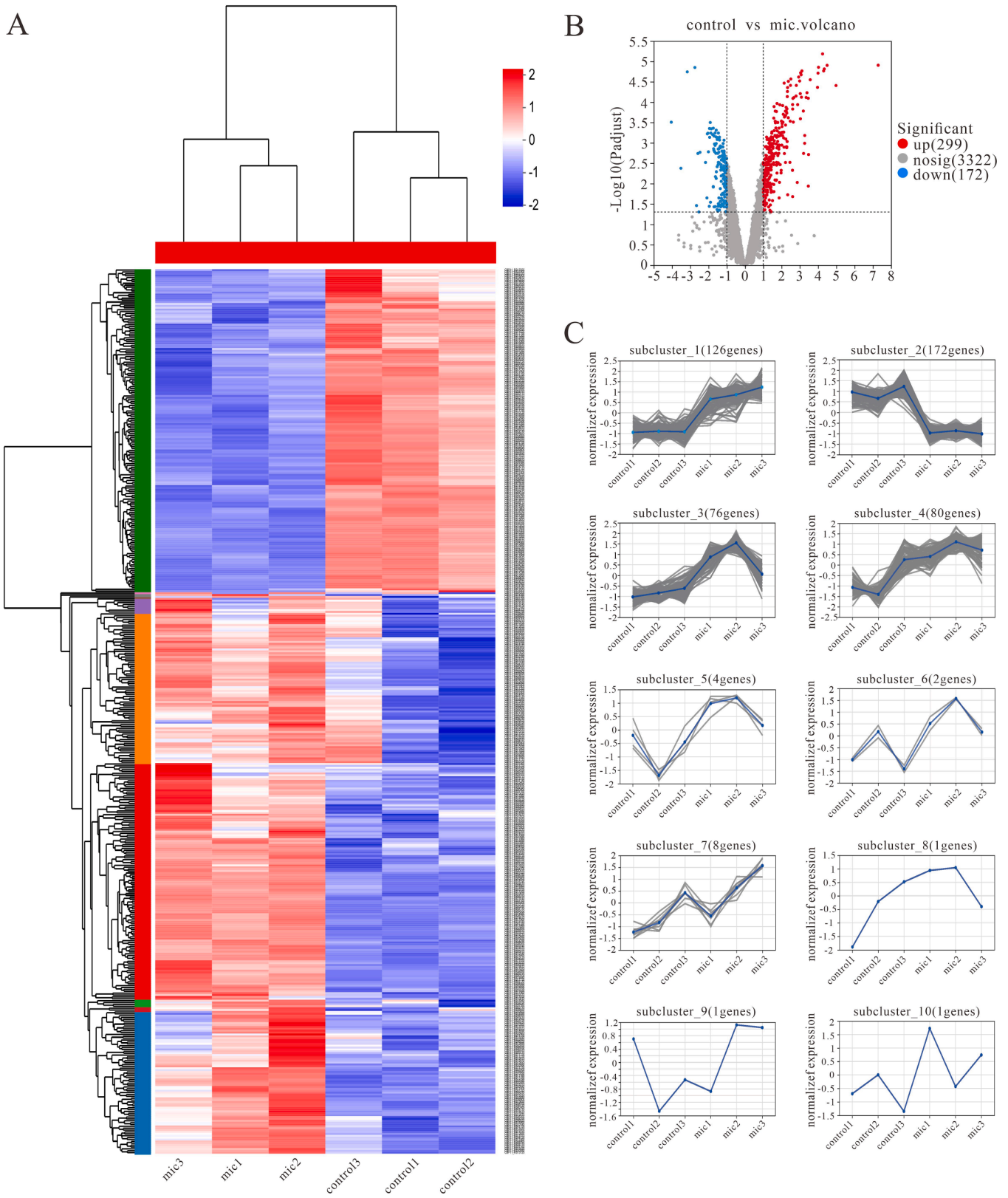

Fig. 3. Differentially expressed genes were compared between the treated (treated with linalool) and the control group (untreated with linalool). (A) Heat map of DEGs. The red cluster represented up-regulated genes, whereas the blue cluster represented down-regulated genes. (B) Volcano plot of DEGs. (C) Line chart with log2 (ratio). The gray lines represented the relative expression of genes in various groups. The average values of the relative expressions of the genes in different groups were shown by the blue lines.

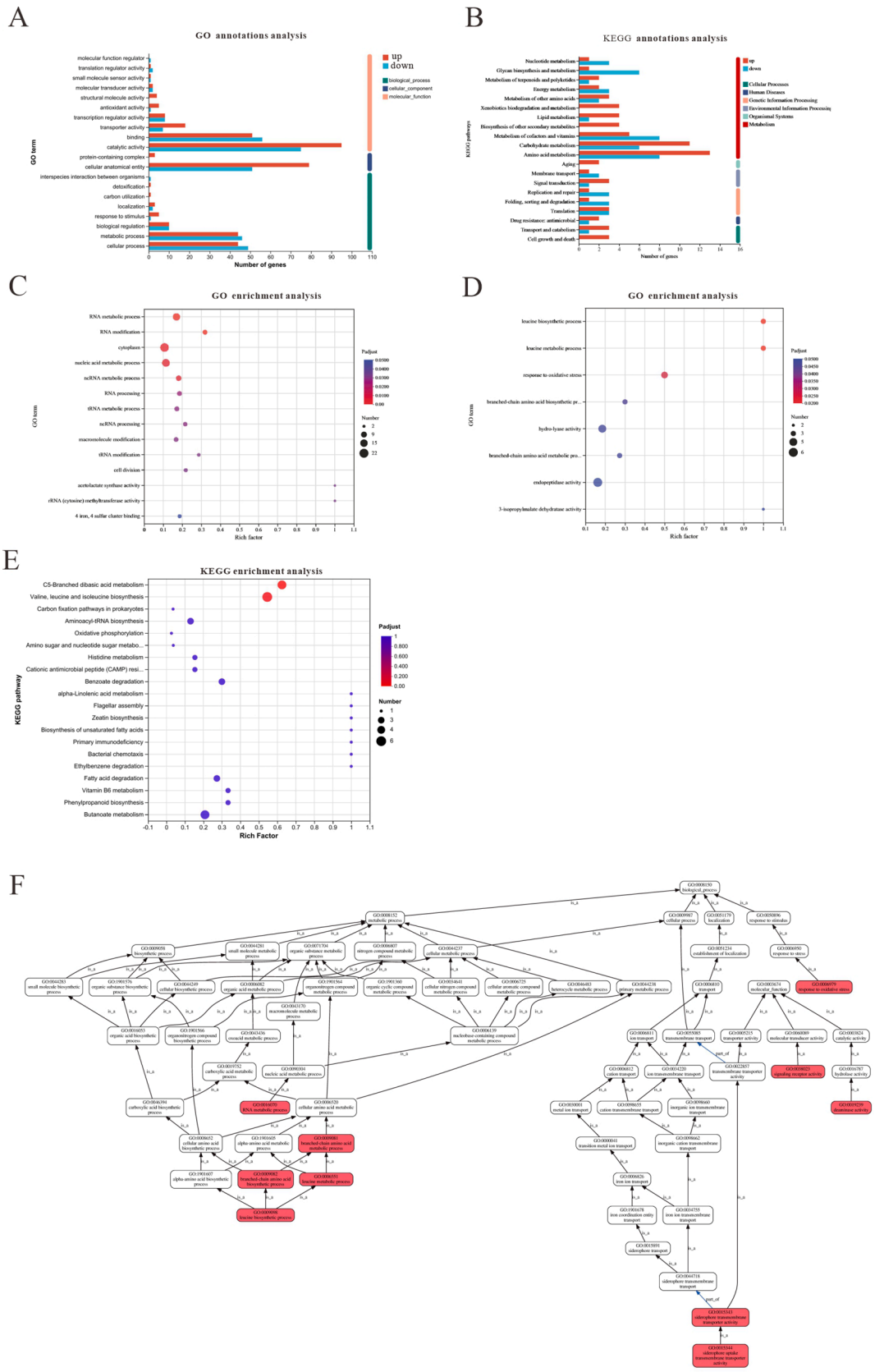

Fig. 4. GO and KEGG analysis between the treated (treated with linalool) and control group (untreated with linalool). (A) GO classification of DEGs. (B) KEGG classification of DEGs. (C) The GO enrichment of down regulated DEGs. (D) The GO enrichment of up regulated DEGs. (E) The KEGG enrichment of regulated DEGs. (F) Hierarchical analysis. Each rectangle represented a different GO item, with the red rectangles highlighting GO items that differ significantly from the others.

2.10. Metabolite sample preparation and metabolomics analysis

Effects of linalool on metabolites and metabolic pathways of *E. miricola* by untargeted metabolomics. Bacterial precipitates cultured to log phase were treated with linalool (0.125 %) for one hour and washed with PBS buffer. The samples were quenched by adding formaldehyde and then placed on ice to prevent any metabolic changes, then the samples were processed and analyzed by UPLC-MS/MS. Metabolomics analysis of raw data obtained by UPLC-MS/MS was performed using Progenesis QI software, including peak comparison, peak extraction, deconvolution, normalization and database search. In order to better analyse the data, the raw data were collated and subjected to multivariate pattern recognition analysis, principal component analysis (PCA) and partial least squares discriminant analysis (PLS-DA) using SIMCA software (V14.1, Sartorius Stedim Data Analytics AB, Umea, Sweden). A PLS-DA model with a cardinality criterion of Fold Change <0.5 or greater than 2, Student's *t*-test with a p-value (P-value) <0.05, and a Variable Importance in the Projection (VIP) of the first principal component of the PLS-DA model greater than Projection, VIP) of the first principal component of the PLS-DA model were considered as differential metabolites. The role of various metabolites and metabolic pathways was investigated by performing KEGG metabolic pathway analysis on the differential metabolites. We defined metabolic pathways as enriched when the ratio $x/n > y/N$ was reached. Metabolic pathways were considered statistically significantly enriched when the p-value of the metabolic pathway was <0.05.

2.11. Statistical analysis

The mean ± standard deviation (SD) of the data is presented. Every experiment was carried out in three duplicates. Data were plotted using the software GraphPad Prism 9.

3. Results

3.1. Antibacterial activity of linalool against E. miricola

The antibacterial activity of linalool against *E. miricola* was shown in Fig. 1. Compared to florfenicol (the ZOI was 31.82 ± 0.62 mm), linalool exhibited similar antibacterial ability, the ZOI, MIC, and MBC were 36.41 ± 1.23 mm, 0.125 % (v/v, 1.0775 mg/mL), 0.125 % (v/v,1.0775 mg/mL), respectively. In addition, we found linalool to be a zone of inhibition for two other *E. miricola* isolates (strain N1 isolated from bullfrogs and strain H1 isolated from black-spotted frogs) (**Figure S1**).

The antimicrobial kinetics of linalool were investigated as shown in Fig. 1**D** The control group showed a typical growth curve consisting of 3 phases: the lag phase (0–4 h), the exponential phase (4–48 h), and the stabilization phase (after 48 h). The 0.25 × MIC-treated group experienced a delay of approximately 2 h during the bacterial stagnation phase relative to the control group, while the OD_{600} value decreased during the plateau phase. In contrast, the 0.5 × MIC treated group exhibited a prolonged bacterial arrest period of around 60 h, which may be attributed to the adaptation time of *E. miricola* to the drug concentration. In addition, the logarithmic cycles were extended for approximately 50 h, indicating a marked decrease in *E. miricola* transient growth acceleration and rate compared to the control group. The 1 × MIC treatment group demonstrated complete inhibition of *E. miricola* growth. The OD_{600} value declined as the linalool concentration increased, suggesting that linalool could limit the maximum environmental capacity of the bacteria in the medium and that its antimicrobial effect increased with higher linalool concentration.

Bacterial survival was indirectly measured by XTT reduction assay after treatment with various linalool concentrations for different time intervals. As shown in Fig. 1C, when treated for up to 2 h with a linalool concentration of 0.25 × MIC, the survival rate of *E. miricola* was approximately 90 %. When treated with 0.5 × MIC linalool, the survival rate of the bacterium gradually decreased with increasing treatment time, and the survival rate of the bacterium was about 50 % at the lowest point. Notably, the survival rate of the bacteria treated with 1 × MIC linalool reached its minimum value after 0.5 h of treatment, and further increases in linalool concentration resulted in a significant acceleration of the instantaneous death rate of the bacteria.

3.2. Effect of linalool on E. miricola morphology

As shown in Fig. 2**A**, the majority of bacteria in the control group were stained green by SYTO 9 fluorescent stain, with only a small amount of red fluorescence observed in the propidium iodide staining, suggesting that the control group was predominantly composed of live bacteria. The presence of some dead bacteria could be attributed to natural apoptosis under normal conditions. In the 0.5 × MIC group, the number of green-stained bacteria in the SYTO 9 staining was notably lower compared to the control group, while the red-stained bacteria in the propidium iodide staining were more pronounced. These observations indicated an increased occurrence of bacterial death at this concentration. When treated with linalool at 1 × MIC, SYTO 9 staining showed no green fluorescence, indicating that the bacteria experienced membrane disruption and could not survive at this concentration. Similarly, the propidium iodide staining revealed an increased presence of red fluorescence in the 1 × MIC group compared to 0.5 × MIC groups. This suggested that as the concentration of linalool increased, the permeability of the bacterial cell membrane was altered, allowing the propidium iodide stain to penetrate the cells. These results indicated that linalool has the potential to compromise the integrity of the bacterial cell membrane.

Electron microscope images (Fig. 2**B**) revealed that *E. miricola* displayed complete round-terminated rods approximately 1 mm in length, with a rough and evenly reticulated surface. When exposed to 1 × MIC linalool for 20, 40, and 60 min, the cell surface exhibited varying degrees of damage. After 20 and 40 min of exposure to 1 × MIC linalool, depressions of various sizes appeared on the bacterial surface. However, no significant difference in bacterial cell volume was observed at this time. Following 60 min of exposure to 1 × MIC linalool, the surface of the bacterial cells crumpled more severely and pores appeared leading to cell volume shrank. These observations suggested that prolonged exposure to linalool led to more pronounced damage and alterations in the bacterial cell structure.

At the start of linalool treatment (0 min), the bacterial structure was intact with a uniform distribution of red and green fluorescence. Following a period of 30 min, the styrene dye FM 4–64 was observed to enter the bacteria, resulting in a gradual increase in red fluorescence penetrate the bacteria. This indicated disruption of the cell wall and cell membrane. The intensity of red fluorescence in bacteria increased with linalool treatment time (Fig. 2**C**), which suggested that prolonged exposure to linalool further exacerbates the damage to the bacterial cell structure.

3.3. Comparative transcriptomic analysis of E. miricola treated and untreated with linalool

Comparative transcriptomic analysis aimed to elucidate the impact of linalool on *E. miricola* at the gene level revealed 471 differentially expressed genes (DEGs) between the control and linalool treatment groups. Among these, 299 genes were up-regulated, while 172 were down-regulated (Fig. 3). Functional characterization of genes and gene products were assessed in detail by gene ontology (GO) analysis (Fig. 4**A**). All DEGs were annotated to one of 20 GO categories, including 10 categories for molecular function, 2 categories for cellular components, and 8 categories for biological activities. The KEGG analysis in Fig. 4**B** classified the DEGs according to the pathway they are involved in or the function they perform. Amino acid metabolism and Carbohydrate metabolism contained the most DEGs in these 7 categories of

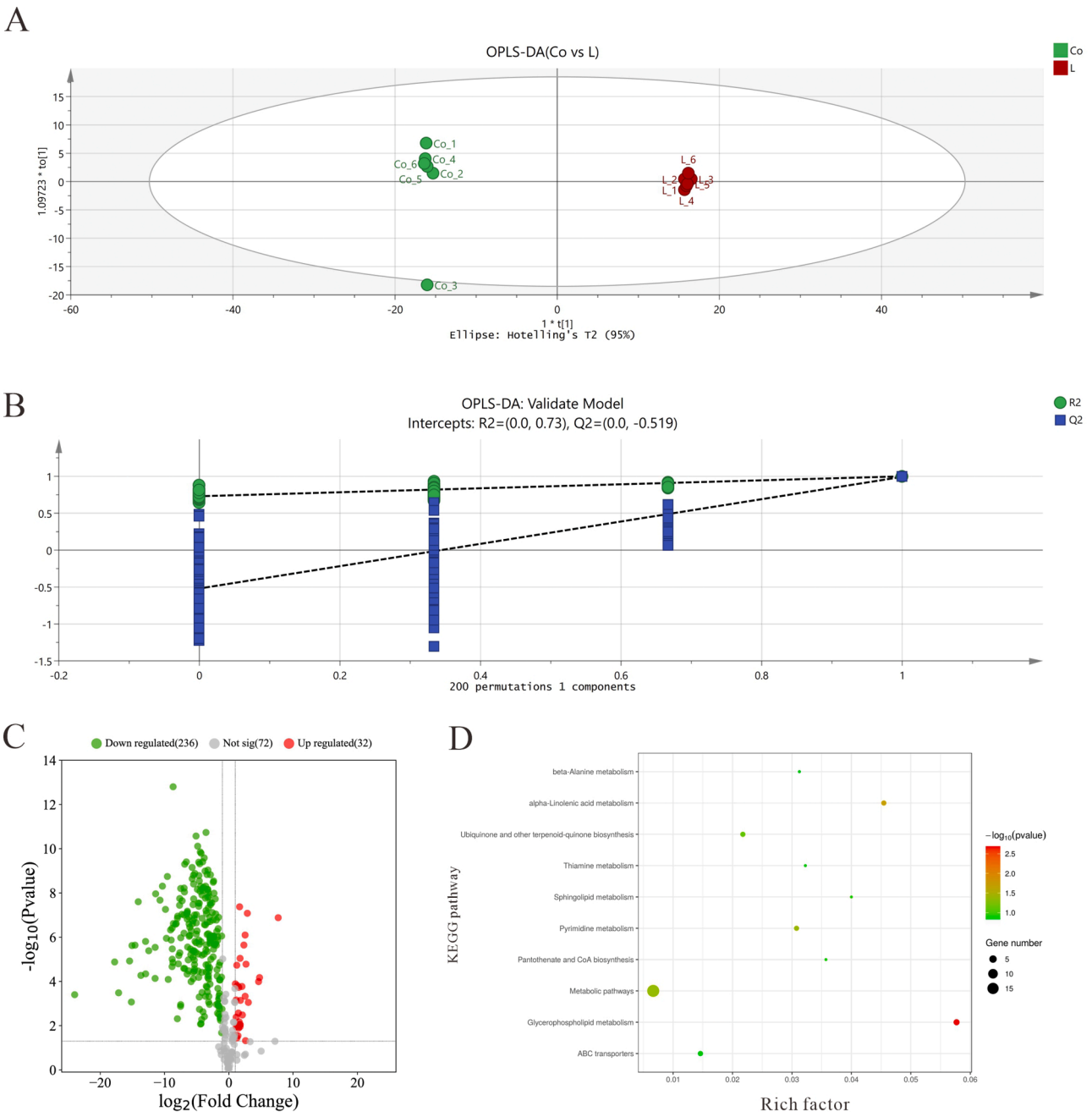

Fig. 5. Multivariate cluster analyses of metabolite profiles of treated and untreated with linalool. (A) OPLS- DA score plot ("Co" Group and "L" Group represented the untreated group and linalool treatment group, respectively). (B) Permutation test of OPLS-DA model. (C) Significantly different metabolite volcano plots for "Co" versus "L" group, red circles indicated ratio Co/*L* > 2, *t*-test p-value<0.05, PLS-DA VIP>1, green circles indicated ratio Co/*L* < 0.5, *t*-test p-value<0.05, PLS-DA VIP>1. (D) Pathway analysis diagram. Each bubble in the bubble diagram represented a metabolic pathway, and the size of the bubble indicates the significantly different metabolite found in that pathway in this experiment; the darker the color of the bubble, the smaller the P-value, and the more significant the enrichment.

pathways.

In order to facilitate the interpretation of these transcriptome results, a GO enrichment analysis was conducted on the top 20 terms in order of enrichment. (Figs. 4**C, D**). Those down regulated biological processes are shown in Fig. 4**C**, we found that 8 process were associated with "RNA", such as the metabolic process of RNA, nucleic acid, ncRNA, and tRNA. Moreover, 5 down regulated DEGs were significantly enriched in the cell division process. Interestingly, 22 down regulated DEGs were significantly enriched in the cytoplasm of cellular components. Those up regulated biological processes was shown in Fig. 4**D**, leucine biosynthesis and metabolic processes enriched for the most DEGs. Moreover, 3 up regulated DEGs were associated with branched-chain amino acid biosynthesis and metabolic processes. Interestingly, 4 up regulated DEGs were associated with bacterial response to oxidative stress processes. The main biological functions of DEGs were shown in Fig. 4**F**. Compared with the control group, the treatment group exhibited significantly different levels of gene expression related to molecular functions, especially the leucine metabolic process (GO:0006,551) and RNA metabolic process (GO:0016,070). When focused on the leucine metabolic process, the branched-chain amino acid metabolic process (GO:0009,081) was associated with it. When focused on the RNA metabolic process, a total of 22 DEGs were enriched in the GO term. For

Table 1
NADP and differential metabolites associated with the glycerophospholipid metabolic pathway.

Compound ID	Description	FC value	P-value	VIP
HMDB0000217	NADP	0.0000574294	<0.001	1.12236
HMDB0010381	LysoPC (15:0)	0.051861794	<0.001	1.03781
HMDB0000520	5a-Cholestane-3a,7a,12a,25-tetrol	0.111216319	<0.001	1.20354
HMDB0009474	PE (20:5(5Z,8Z,11Z,14Z,17Z)/22:6(4Z,7Z,10Z,13Z,16Z,19Z))	0.281734639	<0.05	1.15862
HMDB0113009	PE-NMe (14:1(9Z)/20:5(5Z,8Z,11Z,14Z,17Z))	0.072711714	<0.01	1.01739
HMDB0008910	PE (15:0/22:4(7Z,10Z,13Z,16Z))	0.020113206	<0.001	1.03583
HMDB0009603	PE (22:4(7Z,10Z,13Z,16Z)/22:5(4Z,7Z,10Z,13Z,16Z))	0.004627112	<0.001	1.01921
HMDB0114519	PE-NMe2 (22:4(7Z,10Z,13Z,16Z)/22:5(4Z,7Z,10Z,13Z,16Z))	0.055424076	<0.001	1.03715

the biological process (GO:0008,150), genes associated with it such as response to oxidative stress (GO:0006,979) was altered. For the metabolic processes (GO:0008,152), genes associated with it such as the branched-chain amino acid metabolic process (GO:0009,081) and the leucine biosynthetic process (GO:0009,098) were altered. Meanwhile, the branched-chain amino acid biosynthetic process (GO:0009,082), siderophore uptake transmembrane transporter activity (GO:0015,344), and deaminase activity (GO:0019,239) were also notable impacted.

Moreover, KEGG pathway enrichment analyses were performed to explore the biological functions of the genes at the molecular, cellular, and organismal levels. An enriched bubble chart of candidate genes showed the top 20 most enriched pathways for DEGs (Fig. 4**E**). Among them, c5-branched dibasic acid metabolism and biosynthesis of valine, leucine, and isoleucine were the top 20 most enriched pathways.

3.4. Metabolomics analysisof E. miricola treated and untreated with linalool

The inhibition mechanism of linalool against *E. miricola* was further evaluated by UPLC-MS method. As shown in Fig. 5A, sample differentiation between the control and linalool treatment groups were highly significant, with all samples falling within the 95 % confidence interval (Hotelling's T-squared ellipse). In the OPLS-DA permutation test (Fig. 5**B**), the intercept of the regression line of Q2 was less than zero. Meanwhile, as the replacement retention gradually decreased, the proportion of the replacement Y variable increased, and the Q2 of the random model gradually decreased, implying that the models have good robustness without overfitting. Differential metabolites between control and linalool treatment groups were screened using multivariate statistical analysis of variance and visualized by volcano plots (Fig. 5C). A total of 268 differential metabolites, of which 32 were down regulated and 236 were up regulated. The differential metabolites were annotated into a different pathway through KEGG enrichment analysis. As show in Fig. 5D, the different metabolites were related to beta-alanine metabolism, alpha-Linoleic acid metabolism, ubiquinone and another terpenoid-quinone biosynthesis, thiamine metabolism, sphingolipid metabolism, pyrimidine metabolism, pantothenate, and CoA biosynthesis, metabolic pathways, glycerophospholipid metabolism and ABC transporters. Interestingly, NADP and differential metabolites associated with glycerophospholipids were significantly upregulated (Table 1).

Compound ID denoted the ID of the ingredient in the HMDB database. Description denotes the commonly used chemical name of the ingredient. FC value denotes the ratio of the quantification of the substance in the control group to that in the linalool-treated group. P-value denotes the P-value of the *t*-test between the control group and linalool-treated group, with $P < 0.05$ denoting a significant difference and $P < 0.01$ and $P < 0.001$ indicating difference and significance. VIP indicated VIP value from the PLS-DA model.

4. Discussion

4.1. The antimicrobial activity of essential oils and their main components

Linalool is present in the volatile oils of many naturally occurring aromatic plants and has been widely studied for its high antimicrobial activity. He et al. (He et al., 2022) found that linalool can destroy the cell structure of *Brochothrix thermosphacta*, causing leakage of intracellular material and reported a MIC value of 1.5 mL/L. Tang et al. (Tang et al., 2024) investigated anti-oomycetes activity of linalool against *Saprolegnia ferax* (*S. ferax*) and discovered that linalool exhibited mycelium growth and zoospore production inhibition at 0.1 % (v/v, 0.862 mg/ml) and 0.025 % (v/v, 0.216 mg/ml), respectively. Dias et al. (Dias et al., 2018) determined that the MIC values of linalool on *Candida tropicalis, Candida albicans,* and *Candida krusei* were 500, 1.000, and 2.000 mg/mL, respectively. In our study, linalool showed excellent antimicrobial effect against *E. miricola* with both MIC and MBC values of 0.125 % (v/v, 1.0775 mg/mL). Furthermore, findings revealed that linalool showed strong antimicrobial activity and disrupt the integrity of the cell membrane of *E. miricola*, resulting in leakage of bacterial contents. This observation is consistent with previous studies demonstrating linalool's ability to disrupt bacterial cell membranes. Liu et al. (Liu et al., 2020) observed significant damage to *Pseudomonas aeruginosa* after treatment with linalool with the surface of *P. aeruginosa* appeared to break down over prolonged exposure. Similarly, Gao et al. (Gao et al., 2019) reported that linalool can cause wrinkling of cell membrane in *Listeria monocytogenes* and eventually lead to rupture. He et al. (He et al., 2022) found that the *Brochothrix thermosphacta* appeared deformed and aggregated after treatment with 1 × MIC of linalool, while a 2 × MIC caused hollow and cracked of cell surface. These findings collectively suggest that linalool inhibits bacterial growth by disrupting the cell membrane. To further investigate the antibacterial mechanism of linalool against *E. miricola*, we conducted a comprehensive comparative transcriptomic and metabolomic analysis.

4.2. The comprehensive illustration of important pathways from transcriptomics analyses

Transcriptomics analyses revealed significant changes of DEGs of *E. miricola* response to linalool, particularly C5-branched dibasic acid metabolism and Valine, leucine, and isoleucine biosynthesis. As shown in Fig. 6, the expression of genes *ilvB* and *ilvN* is down-regulated, while the expression of genes *leuC* and *leuD* is up-regulated in the C5-branched-chain dibasic acid metabolic pathway. Down-regulation of *ilvB* and *ilvN* leads to changes in pyruvate, which can enter the tricarboxylic acid cycle for further oxidative catabolism to generate energy. It is hypothesised that the response of *E. miricola* to linalool stress may be energy related. Similarly, pyruvate changes are also observed in the leucine, isoleucine, and valine biosynthetic pathways. Leucine, isoleucine, and valine are branched-chain amino acids (BCAAs) that are synthesized in bacteria, fungi, and plants, but not in mammals, which must obtain them through diet. BCAAs play crucial roles in bacterial

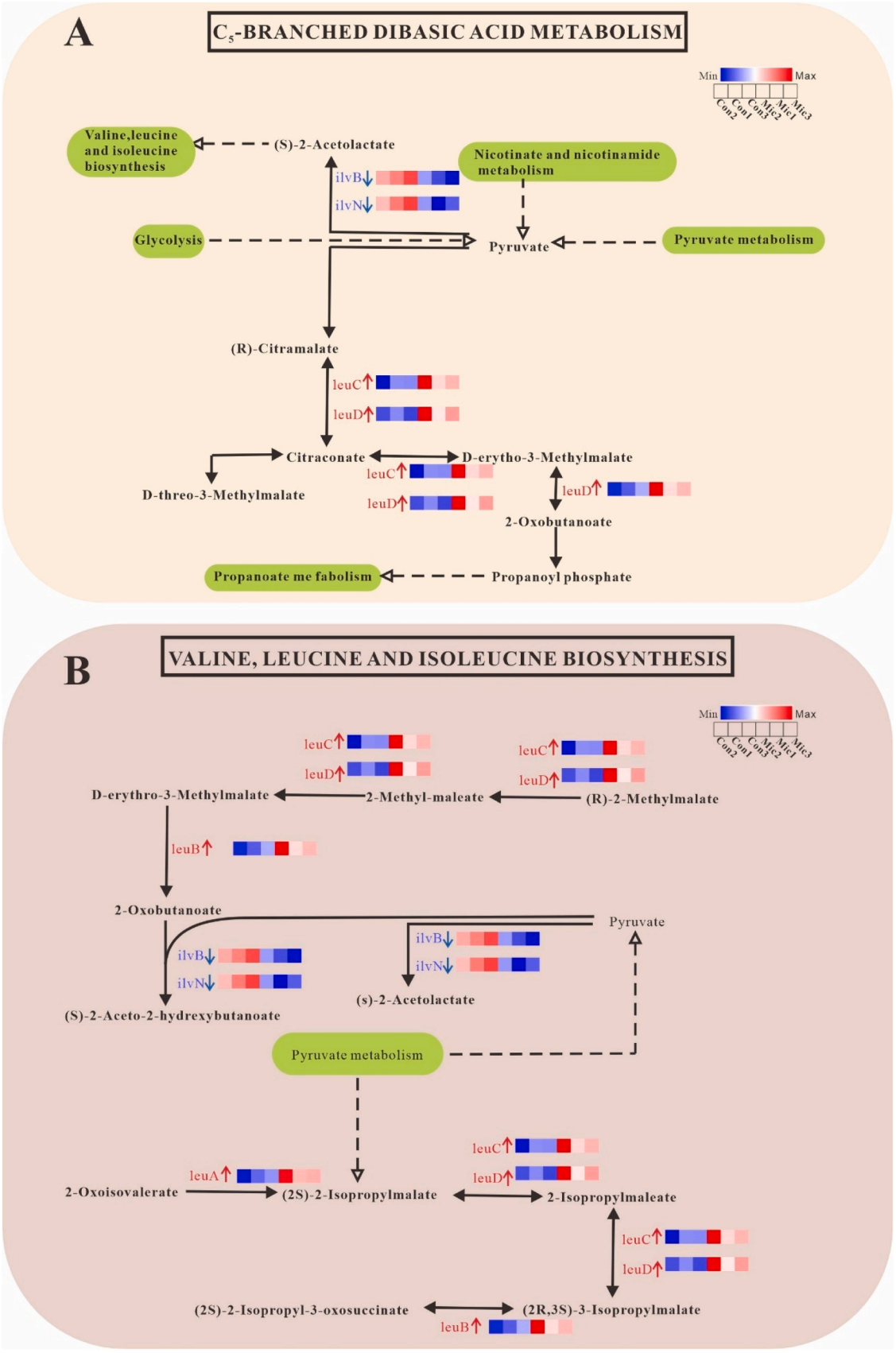

Fig. 6. Important KEGG pathways for DEGs enrichment between treated (linalool-treated group) and control (not linalool-treated) groups. (A) C5-Branched dibasic acid metabolism pathway. (B) Valine, leucine, and isoleucine biosynthesis pathway. Up-regulated genes were indicated by red arrows and down-regulated genes by blue arrows. Square heat maps showed the expression of the relevant DEGs.

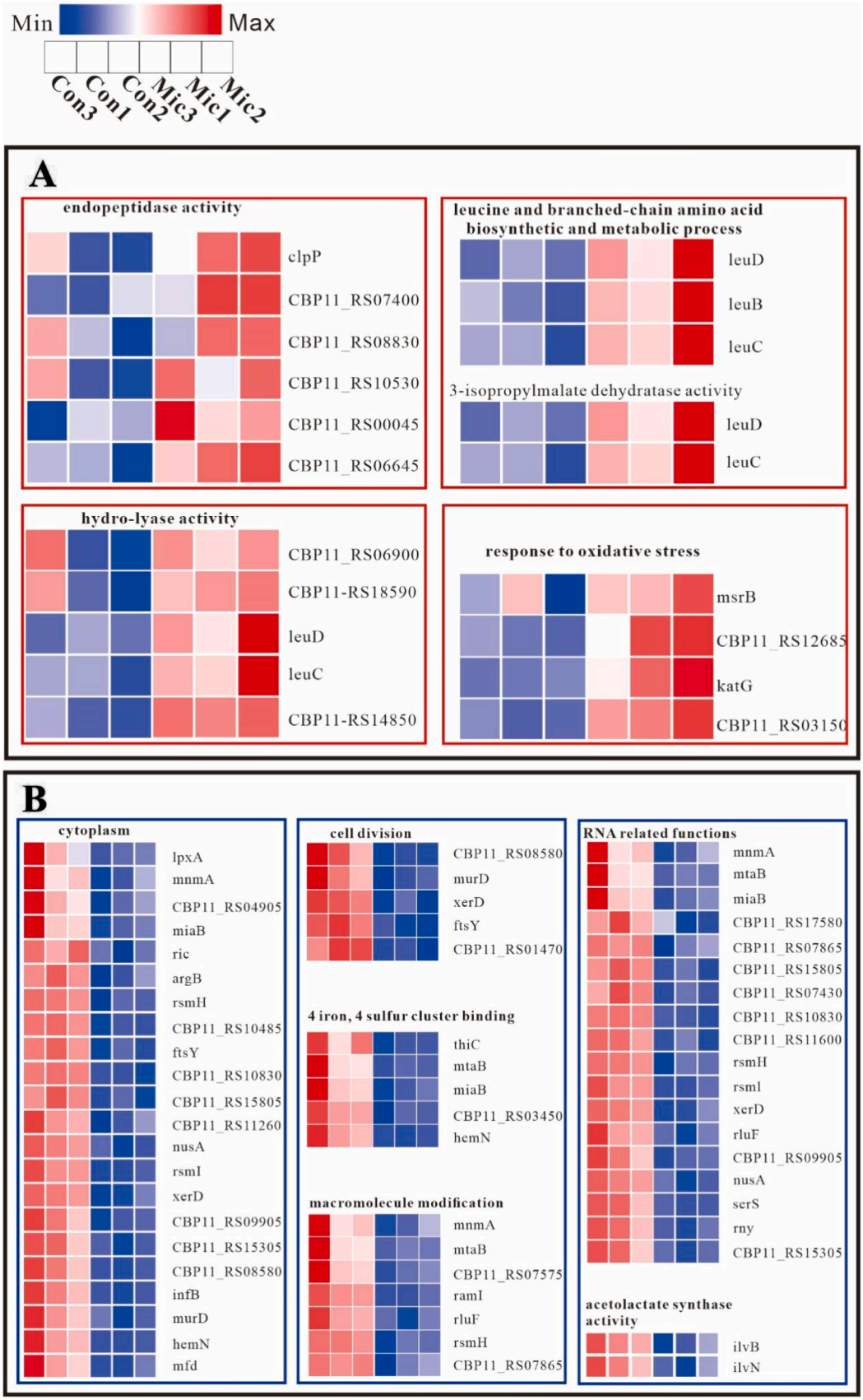

Fig. 7. Heat map of up- and down-regulated genes and their enriched GO functions after linalool treatment. (A) The main gene functions enriched in the up-regulated genes after linalool treatment were endopeptidase activity, leucine and branched-chain amino acid biosynthetic and metabolic process, hydro-lyase activity, and response to oxidative stress. (B) The main gene functions enriched in the down-regulated genes after linalool treatment included RNA-related functions, cytoplasm, cell division, 4 iron, 4 sulfur cluster binding, macromolecule modification and acetolactate synthase activity.

physiology, serving as essential raw materials for protein synthesis and as sources of metabolic energy. For instance, in *Mycobacterium bovine*, the biosynthetic pathways of these BCAAs are critical for the growth and survival of cells (Grandoni et al., 1998). Valenzuela-Miranda et al. demonstrated that when fish rickettsiae are restricted in BCAAs, their growth was inhibited, but this growth limitation can be reversed by supplementing the growth medium with BCAAs (Valenzuela-Miranda and Gallardo-Escárate, 2018). In bacterial cell membranes, isobranched-chain fatty acids and trans-isobranched-chain fatty acids, derived from BCAAs, are major fatty acid species of Bacillus membrane lipids (Mader et al., 2004). In a metabolomic study of the inhibitory activity of glucose and sublethal doses of antibiotics against drug-resistant *S. aureus*, Rutowski J et al. found significant changes in the metabolites of the metabolic pathways of BCAA metabolic pathways, highlighting the impact on the metabolic profiles of drug-resistant *S. aureus* (Rutowski et al., 2019). The diagram of the valine, leucine, and isoleucine biosynthetic pathway is shown in Fig. 6B, illustrating changes in the expression of the genes *leuC, leuD, leuA, leuB, ilvB,* and *ilvN*. Orasch et al. (Orasch et al., 2019) found deletion of the leucine synthase genes *leuA* and *leuC* in *Aspergillus fumigatus* significantly affected fumonisin production and phenotype, primarily impacting iron ion homeostasis and virulence. These findings underscore the importance of BCAAs metabolism in bacterial response to antimicrobial agents and suggest that targeting these pathways could enhance the effectiveness of treatments against resistant bacterial strains.

The main gene functions enriched in the up-regulated genes after linalool treatment were endopeptidase activity, leucine and branched-chain amino acid biosynthetic and metabolic process, hydro-lyase activity, and response to oxidative stress (Fig. 7**A**). The enriched up-regulated genes included *clpP, leuD, leuB, leuC, msrB*, and *katG*. *clpP* gene code ATP-dependent *Clp* endopeptidase proteolytic subunit *ClpP*, which is a serine protease that maintains proteostasis in eukaryotic organelles and prokaryotic cells (Moreno-Cinos et al., 2019). *LeuD, leuB, leuC* encode the small subunit of 3-isopropylmalonate dehydratase, 3-isopropylmalonate dehydrogenase, and the large subunit of 3-isopropylmalonate dehydratase, respectively. It is hypothesized that *E. miricola* obtains large amounts of energy in response to linalool stimulation by up-regulating *claP, leuD, leuC*, and *leuB*. Interestingly, *E. miricola* responds to linalool-induced oxidative stress by up-regulating *msrB* and *katG* genes. *msrB* gene encodes the *MsrB* enzyme, which is capable of reducing methionine-R-sulfoxide and have the ability to protect cellular proteins from oxidative stress damage (Soriani et al., 2009). Zhang et al. (Zhang et al., 2018) found that the *KatG* gene of *A. hydrophila* can help bacteria escape or counteract oxidative stress. Thus, we speculated that *MsrB* and *KatG* genes may be important targets for *E. miricola* resistance to linalool.

The main gene functions enriched in the down-regulated genes after linalool treatment included RNA-related functions, cytoplasm, cell division, 4 iron, 4 sulfur cluster binding, macromolecule modification and acetolactate synthase activity (Fig. 7**B**). Linalool affects the RNA of *E. miricola*, including RNA metabolic process, RNA processing, ncRNA processing, RNA modification, and tRNA processing. Among these, the RNA metabolic process was enriched with the highest number of DEGs, and the major down-regulated genes enriched were *nusA, mtaB, mnmA, miaB, rsmH, rny, serS, rluF rlmB* and *miaA*. *nusA* gene is commonly existed in many bacteria, and the encoded *NusA* protein, which plays an important transcriptional regulatory role in bacteria and is crucial for their normal growth and adaptation to environmental changes. Li et al. (Li et al., 2013) found that *nusA* overexpression enhances host cell resistance to heat shock. *mtaB* gene is a specific gene that encodes MtaB protein, which is involved in various biochemical processes, including methionine biosynthesis and tRNA modification. Arragain et al. (Arragain et al., 2010b) found that MtaB protein has a key role in the conversion of N6-threonylcarbamoyladenosine (t6A) to 2-methylthio-N6-threonylcarbamoyladenosine (ms2t6A). *mnmA* gene encodes a protein known as *MnmA* protein, which is involved in the modification of transfer RNA (tRNA) molecules to ensure accurate and efficient protein synthesis. In vitro synthesis of 2-thiouridine in *Escherichia coli* requires *mnmA* and *IscS* (Kambampati and Lauhon, 2003). *miaB* gene is responsible for encoding an enzyme called tRNA (N6-isopentenyl adenosine(37)-C2)-methylthiotransferase, also known as the MiaB enzyme. The product of the *E. coli* miaB gene is able to participate in methylthiolation of adenosine 37 residue (Arragain et al., 2010a). *rsmH* gene encodes RsmH enzyme, a 16S rRNA (cytosine (1402)-N (4))-methyltransferase. Wei et al. (Wei et al., 2012) found that compared to wild-type *E. coli, rsmH* knockout (*ΔrsmH*) strains showed an increase growth rate in doubling time of approximately 12 %, suggesting that the modification defect affects cell growth characteristics. *rny* gene, also known as the *RNAse Y* gene, was found to influence mRNA expression and play a significant role in the coordinated activation of virulence genes in *S. aureus* (Marincola et al., 2012).

The *serS* gene encodes the seryl aminoacyl-tRNA synthetase, overexpression of the *serS* rescues growth defects in *E. coli* caused by the loss of the gene encoding the RarA protein (Jain et al., 2022). *rluF* gene encodes pseudo uridine synthase, which catalyzes the formation of pseudo uridine at position 11,921 in 23S rRNA. *miaA* gene encodes the MiaA enzyme (tRNA (adenosine(37)-N6)-dimethylallyl transferase), Oksana et al. (Koshla et al., 2019) found that Streptomyces albus deletion of the *miaA* gene was observed to have significant growth defects and slow aerial hyphae formation, thereby delaying spore formation. As such, linalool might inhibit the vital activity of *E. miricola* by affecting its RNA processes. Additionally, linalool also affected cell division in *E. miricola*, leading to down-regulation of genes such as *murD, xerD, ftsY*. It is hypothesised that linalool might inhibit the growth and reproduction of *E. miricola* by affecting its cell division.

4.3. The comprehensive illustration of important pathways from metabolomic analyses

The use of metabolomics enabled further evaluation of the inhibitory mechanism of linalool against *E. miricola* from a metabolic perspective. In our study, significant changes in the metabolites of *E. miricola* were observed after treatment with linalool. Notably, the enriched differential metabolites were associated with glycerophospholipid metabolism. Glycerophospholipids are major components of bacterial cell membranes and are essential for protecting bacteria from environmental stress (Jeyaraj et al., 2023). Our results showed a significant up-regulation of several metabolites related to glycerophospholipid metabolism (Table 1). Similarly, *P.anomala* showed an increase in phosphatidylcholine ((PC (18:0/0:0), PC (16:0/0:0), PC (15:0/0:0), LysoPC (18:0), LysoPC (16:0) and LysoPC (14:0/0:0)) content of the glycerophospholipid pathway under ethanol stress (Chen et al., 2023). Reports indicated that the metabolite levels of the glycerophospholipid metabolic pathway were significantly up-regulated under hypoxic stress in *S. cerevisiae*, may maintain the stability of the cellular membranes against the hypoxic stress to mitigate cellular damage and to sustain the survival of cells and to produce energy (Xia et al., 2019). *Candida glabrata Yak1* recruits *Med2* by activating *Yap6*, thereby increasing glycerophospholipid content and membrane integrity and conferring low pH stress tolerance (Zhou et al., 2020). Meanwhile, Phosphorylated *Rds2* plays an important role in increasing glycerophospholipid composition and membrane integrity under osmotic stress in *C. glabrata*, thereby promoting cell growth and survival (Wu et al., 2019). Our study found that linalool disrupted the cell membrane of *E. miricola*, so we hypothesized that *E. miricola* responded to linalool-induced cell membrane damage by producing lipid components. Metabolomic results also found that the linalool-treated group showed a significant increase of nicotinamide adenine dinucleotide phosphate NADP content (Table 1), which is an important cofactor maintaining intracellular redox potential and is involved in glycolysis (Liu et al., 2016). The elevated NADP content may be an important metabolic response of *E. miricola* to linalool stress.

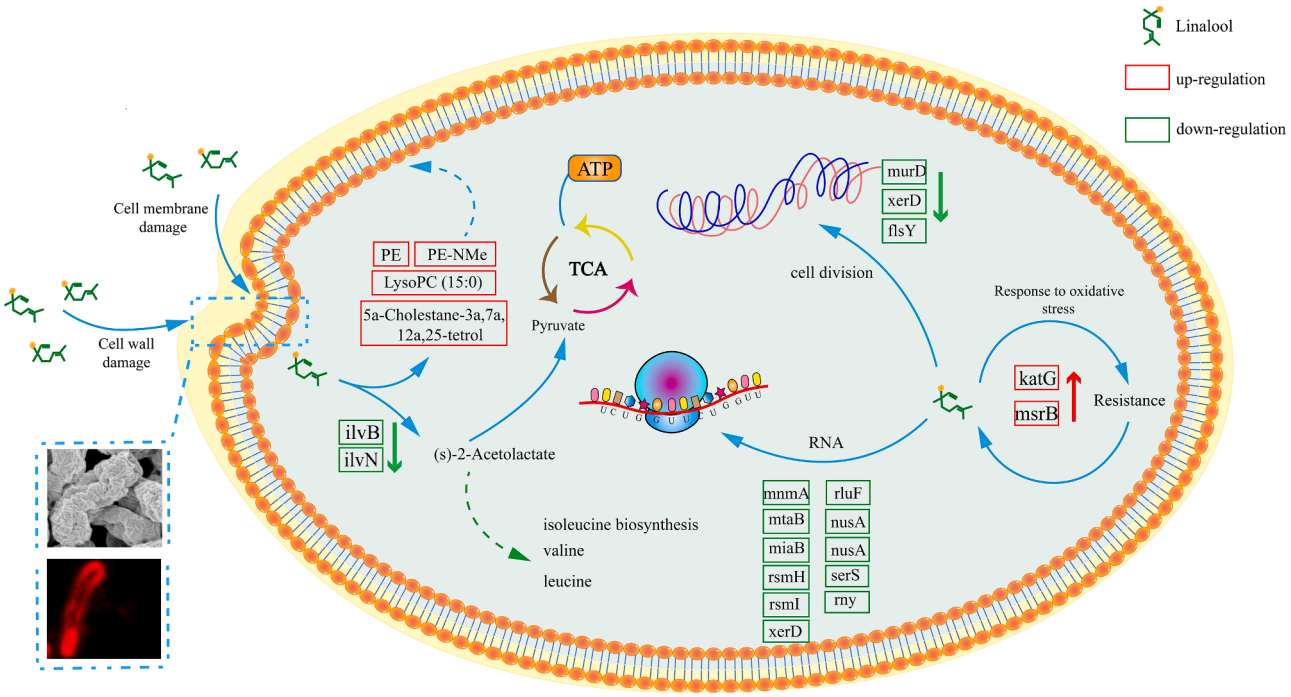

Fig. 8. Model diagram of the mode of action of linalool against *E. miricola*.

5. Conclusions

In conclusion, our results demonstrated that linalool exhibited effective antibacterial activity against *E. miricola*. Linalool disrupted membrane integrity, causing membrane damage and rupture. The antimicrobial mechanism of linalool against *E. miricola* is shown in Fig. 8. Linalool treatment impacted several metabolic pathways, including C5-branched dibasic acid metabolism, Valine, leucine, and isoleucine biosynthesis, RNA, cell division, and response to oxidative stress. For the metabolomic level, linalool influenced glycerophospholipid metabolic pathways and increased NADP content in *E. miricola*. These findings provide a theoretical basis for understanding the antibacterial mechanism of linalool and suggest its potential application in preventing *E. miricola* infections. Future work will involve using black-spotted frogs as a disease model to conduct in vivo studies and developing linalool-loaded nanostructured lipid carriers for targeted treatment, further evaluating the practical applicability of linalool as an antimicrobial agent.

Credit author statement

Mingwang He: Writing - original draft, Conceptualization, Methodology. Weiming Zhong: Data curation, Methodology. RongsiDai: Data curation. Ying Zhou: Data curation. Tongping Zhang: Data curation. Boyang Zhou: Methodology. Tao Tang: Methodology. Linlin Yang: Methodology. Sifan Jiang: Methodology. Wenbin Xiao Methodology. YanJiao Fu Methodology. Jiajing Guo: Writing - review & editing. Zhipeng Gao: Writing - review & editing, Funding acquisition, Supervision. All authors agree to be accountable for all aspects of the work.

Declaration of competing interest

All authors declare that they have no known competing financial interests or personal relationships that could have appeared to influence the work reported in this paper.

Acknowledgments

This research was funded by Hunan Provincial Natural Science Foundation (2025JJ50171, 2023JJ40364), National Natural Science Foundation of China (32073020, 32201960), Science and Technology Innovation Program of Hunan Province (2022RC1150).

Supplementary materials

Supplementary material associated with this article can be found, in the online version, at doi:10.1016/j.crmicr.2025.100380.

Data availability

Data will be made available on request.

References

Abd El-BakyZ.S. Hashem, R.M., 2016. Eugenol and linalool: comparison of their antibacterial and antifungal activities. Afr. J. Microbiol. Res. 10 (44), 1860–1872. https://doi.org/10.5897/AJMR2016.8283.

Arragain, S., Handelman, S.K., Forouhar, F., Wei, F.-Y., Tomizawa, K., Hunt, J.F., Douki, T., Fontecave, M., Mulliez, E., Atta, M., 2010a. Enzymatic modification of tRNAs: miaB is an iron-sulfur protein. J. Biol. Chem. 285 (37), 28425–28433. https://doi.org/10.1074/jbc.C100609200.

Arragain, S., Handelman, S.K., Forouhar, F., Wei, F.-Y., Tomizawa, K., Hunt, J.F., Douki, T., Fontecave, M., Mulliez, E., Atta, M., 2010b. Identification of eukaryotic and prokaryotic methylthiotransferase for biosynthesis of 2-methylthio-N6-threonylcarbamoyladenosine in tRNA. J. Biol. Chem. 285 (37), 28425–28433. https://doi.org/10.1074/jbc.M110.106831.

Badawi, K., Deskins, S., Catherman, K., Lastinger, A., 2022. Out of this world: *elizabethkingia miricola* complicated urinary tract infection in a patient with associated pubic symphysis osteomyelitis and pyomyositis. IDCases 29, e01573. https://doi.org/10.1016/j.idcr.2022.e01573.

Breurec, S., Criscuolo, A., Diancourt, L., Rendueles, O., Vandenbogaert, M., Passet, V., Caro, V., Rocha, E.P.C., Touchon, M., Brisse, S., 2016. Genomic epidemiology and global diversity of the emerging bacterial pathogen *Elizabethkingia anophelis*. Sci. Rep. 6, 12. https://doi.org/10.1038/srep30379.

Bulagonda, E.P., Manivannan, B., Mahalingam, N., Lama, M., Chanakya, P.P., Khamari, B., Jadhao, S., Vasudevan, M., Nagaraja, V., 2018. Comparative genomic analysis of a naturally competent *Elizabethkingia anophelis* isolated from an eye infection. Sci. Rep. 8, 10. https://doi.org/10.1038/s41598-018-26874-8.

Calatrava, E., Casanovas, I., Foronda, C., Cobo, F., 2020. Joint infection due to *Elizabethkingia miricola*. Rev. Esp. Quim 33 (2), 141–142. https://doi.org/10.37201/req/081.2019.

Chen, Y.R., Wan, Y., Cai, W.Q., Che, X.M., Sun, X.H., Peng, H., Luo, H.B., Huang, D., Fu, G.M., 2023. Transcriptomic and metabonomic to evaluate the effect mechanisms of the growth and aroma-producing of *Pichia anomala* under ethanol stress. Food Biosci. 56, 10. https://doi.org/10.1016/j.fbio.2023.103176.

Colapietro, M., Endimiani, A., Sabatini, A., Marcoccia, F., Celenza, G., Segatore, B., Amicosante, G., Perilli, M., 2016. BlaB-15, a new BlaB metallo-β-lactamase variant found in an *Elizabethkingia miricola* clinical isolate. Diagn. Microbiol. Infect. Dis. 85 (2), 195–197. https://doi.org/10.1016/j.diagmicrobio.2015.11.016.

Dias, I.J., Trajano, E., Castro, R.D., Ferreira, G.L.S., Medeiros, H.C.M., Gomes, D.Q.C., 2018. Antifungal activity of linalool in cases of *Candida* spp. Isolated from individuals with oral candidiasis. Braz. J. Biol. 78 (2), 368–374. https://doi.org/10.1590/1519-6984.171054.

Doijad, S., Ghosh, H., Glaeser, S., Kämpfer, P., Chakraborty, T., 2016. Taxonomic reassessment of the genus *Elizabethkingia* using whole-genome sequencing: *elizabethkingia endophytica* Kämpfer et al. 2015 is a later subjective synonym of *Elizabethkingia anophelis* Kämpfer et al. 2011. Int. J. Syst. Evol. Microbiol. 66, 4555–4559. https://doi.org/10.1099/ijsem.0.001390.

Elbe, H., Ozturk, F., Yigitturk, G., Baygar, T., Cavusoglu, T., 2022. Anticancer activity of linalool: comparative investigation of ultrastructural changes and apoptosis in breast cancer cells. Ultrastruct. Pathol. 46 (4), 348–358. https://doi.org/10.1080/01913123.2022.2091068.

Gao, H.G., Li, T., Feng, L., Zhang, S., 2021. *Elizabethkingia miricola* causes intracranial infection: a case study. Front Med 8, 6. https://doi.org/10.3389/fmed.2021.761924.

Gao, Z.P., Van Nostrand, J.D., Zhou, J.Z., Zhong, W.M., Chen, K.Y., Guo, J.J., 2019. Anti-listeria activities of linalool and its mechanism revealed by comparative transcriptome analysis. Front. Microbiol. 10, 13. https://doi.org/10.3389/fmicb.2019.02947.

Grandoni, J.A., Marta, P.T., Schloss, J.V., 1998. Inhibitors of branched-chain amino acid biosynthesis as potential antituberculosis agents. J. Antimicrob. Chemother. 42 (4), 475–482. https://doi.org/10.1093/jac/42.4.475.

Green, O., Murray, P., Gea-Banacloche, J.C., 2008. Sepsis caused by *Elizabethkingia miricola* successfully treated with tigecycline and levofloxacin. Diagn. Microbiol. Infect. Dis. 62 (4), 430–432. https://doi.org/10.1016/j.diagmicrobio.2008.07.015.

Guo, F.Y., Liang, Q., Zhang, M., Chen, W.X., Chen, H.M., Yun, Y.H., Zhong, Q.P., Chen, W.J., 2021a. Antibacterial activity and mechanism of linalool against *Shewanella putrefaciens*. Molecules 26 (1), 17. https://doi.org/10.3390/molecules26010245.

Guo, F.Y., Chen, Q.P., Liang, Q., Zhang, M., Chen, W.X., Chen, H.M., Yun, Y.H., Zhong, Q. P., Chen, W.J., 2021b. Antimicrobial activity and proposed action mechanism of linalool against *Pseudomonas fluorescens*. Front. Microbiol. 12, 11. https://doi.org/10.3389/fmicb.2021.562094.

Gupta, P., Zaman, K., Mohan, B., Taneja, N., 2017. *Elizabethkingia miricola*: a rare non-fermenter causing urinary tract infection. World J Clin Cases 5 (5), 187–190. https://doi.org/10.12998/wjcc.v5.i5.187.

He, R.R., Zhong, Q.P., Chen, W.J., Zhang, M., Pei, J.F., Chen, H.M., Chen, W.X., 2022. Antimicrobial mechanism of linalool against *Brochothrix thermosphacta* and its application on chilled beef. Food Res. Int. 157, 12. https://doi.org/10.1016/j.foodres.2022.111407.

Howard, J.C., Chen, K., Anderson, T., Dalton, S.C., 2020. *Elizabethkingia miricola* bacteraemia in a haemodialysis patient. Access Microbiol 2 (2), acmi000098. https://doi.org/10.1099/acmi.0.000098.

Hu, R.X., Yuan, J.F., Meng, Y., Wang, Z., Gu, Z.M., 2017. Pathogenic *Elizabethkingia miricola* Infection in Cultured Black-Spotted Frogs, 23. Emerg Infect Dis, China, pp. 2055–2059. https://doi.org/10.3201/eid2312.170942, 2016.

Hwang, J.H., Kim, J., Kim, J.H., Mo, S., 2021. *Elizabethkingia argenteiflava* sp. nov., isolated from the pod of soybean, *glycine* max. Int. J. Syst. Evol. Microbiol. 71 (4), 8. https://doi.org/10.1099/ijsem.0.004767.

Jain, K., Stanage, T.H., Wood, E.A., Cox, M.M., 2022. The *Escherichia coli serS* gene promoter region overlaps with the *rarA* gene. PLoS One 17 (4), 14. https://doi.org/10.1371/journal.pone.0260282.

Jeyaraj, E.J., Han, M.-L., Li, J., Choo, W.S., 2023. Metabolic perturbations and key pathways associated with the bacteriostatic activity of *Clitoria ternatea* flower anthocyanin fraction against *Escherichia coli*. Access Microbiol 5 (6). https://doi.org/10.1099/acmi.0.000535.v5.

KambampatiC.T. Lauhon, R., 2003. MnmA and IscS are required for in vitro 2-thiouridine biosynthesis in *Escherichia coli*. Biochemistry 42 (4), 1109–1117. https://doi.org/10.1021/bi026536+.

Kämpfer, P., Matthews, H., Glaeser, S.P., Martin, K., Lodders, N., Faye, I., 2012. *Elizabethkingia anophelis* sp. nov., isolated from the midgut of the mosquito Anopheles gambiae. Int. J. Syst. Evol. Microbiol. 62. https://doi.org/10.1099/ijs.0.68148-0, 1016-1016.

Kim, K.K., Kim, M.K., Lim, J.H., Park, H.Y., Lee, S.-T., 2005. Transfer of *chryseobacterium meningosepticum* and *chryseobacterium miricola* to *Elizabethkingia* gen. nov. As *Elizabethkingia meningoseptica* comb. nov. And *Elizabethkingia miricola* comb. nov. Int. J. Syst. Evol. Microbiol. 55 (Pt 3), 1287–1293. https://doi.org/10.1099/ijs.0.63541-0.

Kim, M.G., Kim, S.M., Min, J.H., Kwon, O.K., Park, M.H., Park, J.W., Ahn, H.I., Hwang, J. Y., Oh, S.R., Lee, J.W., Ahn, K.S., 2019. Anti-inflammatory effects of linalool on ovalbumin-induced pulmonary inflammation. Int. Immunopharmacol. 74, 9. https://doi.org/10.1016/j.intimp.2019.105706.

King, E.O., 1959. Studies on a group of previously unclassified bacteria associated with meningitis in infants. Am. J. Clin. Pathol. 31 (3), 241–247. https://doi.org/10.1093/ajcp/31.3.241.

Kisacam, M.A., Sakin, F., Irtegun-Kandemir, S., Pektanc-Sengul, G., Kurekci, C., 2022. Linalool and eugenol exhibit apoptotic potential on hela and caco-2 cells through the modulation of src kinases and ADAMTS proteases while only eugenol displays anti-angiogenic features on HeLa cells. Biologia (Bratisl) 77 (3), 865–877.

Koshla, O., Yushchuk, O., Ostash, I., Dacyuk, Y., Myronovskyi, M., Jäger, G., Süssmuth, R.D., Luzhetskyy, A., Byström, A., Kirsebom, L.A., 2019. Gene *miaA* for post-transcriptional modification of $tRNA_{XXA}$ is important for morphological and metabolic differentiation in *streptomyces*. Mol. Microbiol. 112 (1), 249–265. https://doi.org/10.1111/mmi.14266.

Lau, S.K.P., Chow, W.N., Foo, C.H., Curreem, S.O.T., Lo, G.C.S., Teng, J.L.L., Chen, J.H. K., Ng, R.H.Y., Wu, A.K.L., Cheung, I.Y.Y., Chau, S.K.Y., Lung, D.C., Lee, R.A., Tse, C. W.S., Fung, K.S.C., Que, T.L., Woo, P.C.Y., 2016. *Elizabethkingia anophelis* bacteremia is associated with clinically significant infections and high mortality. Sci. Rep. 6, 10. https://doi.org/10.1038/srep26045.

Lei, X.P., Yi, G., Wang, K.Y., OuYang, P., Chen, D.F., Huang, X.L., Huang, C., Lai, W.M., Zhong, Z.J., Huo, C.L., Yang, Z.X., 2019. *Elizabethkingia miricola* infection in Chinese spiny frog (*Quasipaa spinosa*). Transbound Emerg Dis 66 (2), 1049–1053. https://doi.org/10.1111/tbed.13101.

Li, K., Jiang, T., Yu, B., Wang, L., Gao, C., Ma, C., Xu, P., Ma, Y., 2013. *Escherichia coli* transcription termination factor NusA: heat-induced oligomerization and chaperone activity. Sci. Rep. 3 (1), 2347. https://doi.org/10.1038/srep02347.

Li, Y., Ren, F., Chen, D., Chen, H., Chen, W., 2022. Antibacterial mechanism of Linalool against *Pseudomonas fragi*: a transcriptomic study. Foods 11 (14), 2058. https://doi.org/10.3390/foods11142058.

Li, Y., Kawamura, Y., Fujiwara, N., Naka, T., Liu, H., Huang, X., Kobayashi, K., Ezaki, T., 2003. *Chryseobacterium miricola* sp. nov., a novel species isolated from condensation water of space station Mir. Syst. Appl. Microbiol. 26 (4), 523–528. https://doi.org/10.1078/072320203770865828.

Lima, M.I.D., de Medeiros, A.C.A., Silva, K.V.S., Cardoso, G.N., Lima, E.D., Pereira, F.D., 2017. Investigation of the antifungal potential of linalool against clinical isolates of fluconazole resistant *trichophyton rubrum*. J. Mycol. Med 27 (2), 195–202. https://doi.org/10.1016/j.mycmed.2017.01.011.

Lin, J.N., Lai, C.H., Yang, C.H., Huang, Y.H., Lin, H.F., Lin, H.H., 2017. Comparison of four automated microbiology systems with 16S rRNA gene sequencing for identification of *chryseobacterium* and *Elizabethkingia* species. Sci. Rep. 7, 5. https://doi.org/10.1038/s41598-017-14244-9.

Liu, X.-X., Liu, W.-b., Ye, B.-C., 2016. Regulation of a protein acetyltransferase in *myxococcus xanthus* by the coenzyme $NADP^+$. J. Bacteriol. 198 (4), 623–632. https://doi.org/10.1128/JB.00661-15.

Liu, X., Cai, J.X., Chen, H.M., Zhong, Q.P., Hou, Y.Q., Chen, W.J., Chen, W.X., 2020. Antibacterial activity and mechanism of linalool against *Pseudomonas aeruginosa*. Microb. Pathog. 141. https://doi.org/10.1016/j.micpath.2020.103980.

Mączka, W., Duda-Madej, A., Grabarczyk, M., Wińska, K., 2022. Natural compounds in the battle against microorganisms—Linalool. Molecules 27 (20), 6928. https://doi.org/10.3390/molecules27206928.

Mader, U., Hennig, S., Hecker, M., Homuth, G., 2004. Transcriptional organization and posttranscriptional regulation of the *Bacillus subtilis* branched-chain amino acid biosynthesis genes. J. Bacteriol. 186 (8), 2240–2252. https://doi.org/10.1128/jb.186.8.2240-2252.2004.

Marincola, G., Schäfer, T., Behler, J., Bernhardt, J., Ohlsen, K., Goerke, C., Wolz, C., 2012. RNase Y of *Staphylococcus aureus* and its role in the activation of virulence genes. Mol. Microbiol. 85 (5), 817–832. https://doi.org/10.1111/j.1365-2958.2012.08144.x.

Moreno-Cinos, C., Goossens, K., Salado, I.G., Van Der Veken, P., De Winter, H., Augustyns, K., 2019. ClpP protease, a promising antimicrobial target. Int. J. Mol. Sci. 20 (9), 19. https://doi.org/10.3390/ijms20092232.

Opota, O., Diene, S.M., Bertelli, C., Prod'hom, G., Eckert, P., Greub, G., 2017. Genome of the carbapenemase-producing clinical isolate *Elizabethkingia miricola* EM_CHUV and comparative genomics with *Elizabethkingia meningoseptica* and *Elizabethkingia anophelis*: evidence for intrinsic multidrug resistance trait of emerging pathogens. Int. J. Antimicrob. Agents 49 (1), 93–97. https://doi.org/10.1016/j.ijantimicag.2016.09.031.

Orasch, T., Dietl, A.M., Shadkchan, Y., Binder, U., Bauer, I., Lass-Flörl, C., Osherov, N., Haas, H., 2019. The leucine biosynthetic pathway is crucial for adaptation to iron starvation and virulence in *Aspergillus fumigatus*. Virulence 10 (1), 925–934. https://doi.org/10.1080/21505594.2019.1682760.

Parvekar, P., Palaskar, J., Metgud, S., Maria, R., Dutta, S., 2020. The minimum inhibitory concentration (MIC) and minimum bactericidal concentration (MBC) of silver nanoparticles against *Staphylococcus aureus*. Biomater Invest Dent 7 (1), 105–109. https://doi.org/10.1080/26415275.2020.1796674.

Peng, S.Y., Chen, L.K., Wu, W.J., Paramita, P., Yang, P.W., Li, Y.Z., Lai, M.J., Chang, K.C., 2020. Isolation and characterization of a new phage infecting *Elizabethkingia anophelis* and evaluation of its therapeutic efficacy in vitro and in vivo. Front. Microbiol. 11, 10. https://doi.org/10.3389/fmicb.2020.00728.

Penven, M., Lalieu, A., Boruchowicz, A., Paluch, M., Diedrich, T., Dewulf, G., Cattoen, C., 2020. Bacteremia caused by *Elizabethkingia miricola* in a patient with acute pancreatitis and peritoneal dialysis. Med. Mal. Infect. 50 (4), 379–381. https://doi.org/10.1016/j.medmal.2020.01.009.

Rossati, A., Kroumova, V., Bargiacchi, O., Brustia, D., Garavelli, P.L., 2015. *Elizabethkingia miricola* bacteriemia in a young woman with acute alcoholic pancreatitis. Presse Med. 44 (10), 1071–1072. https://doi.org/10.1016/j.lpm.2015.08.003.

Rutowski, J., Zhong, F.Y., Xu, M.Y., Zhu, J.J., 2019. Metabolic shift of *Staphylococcus aureus* under sublethal dose of methicillin in the presence of glucose. J. Pharm. Biomed. Anal. 167, 140–148. https://doi.org/10.1016/j.jpba.2019.02.010.

Shirmast, P., Ghafoori, S.M., Irwin, R.M., Abendroth, J., Mayclin, S.J., Lorimer, D.D., Edwards, T.E., Forwood, J.K., 2021. Structural characterization of a GNAT family acetyltransferase from *Elizabethkingia anophelis* bound to acetyl-CoA reveals a new dimeric interface. Sci. Rep. 11 (1), 9. https://doi.org/10.1038/s41598-020-79649-5.

Soriani, F.M., Kress, M.R., de Gouvêa, P.F., Malavazi, I., Savoldi, M., Gallmetzer, A., Strauss, J., Goldman, M.H.S., Goldman, G.H., 2009. Functional characterization of the Aspergillus nidulans methionine sulfoxide reductases (msrA and msrB). Fung. Genet. Biol. 46 (5), 410–417. https://doi.org/10.1016/j.fgb.2009.01.004.

Su, R., Guo, P., Zhang, Z., Wang, J., Guo, X., Guo, D., Wang, Y., Lü, X., Shi, C., 2022. Antibacterial activity and mechanism of Linalool against *Shigella sonnei* and its application in lettuce. Foods 11 (20), 3160. https://doi.org/10.3390/foods11203160.

Tang, T., Zhong, W.M., Yang, L.L., He, M.W., Jiang, S.F., Yin, D., Guo, J.J., Gao, Z.P., 2024. In vitro and in vivo anti-oomycetes activities and mechanisms of linalool against *Saprolegnia ferax*. Aquaculture 578, 13. https://doi.org/10.1016/j.aquaculture.2023.740031.

Valenzuela-MirandaC. Gallardo-Escárate, D., 2018. Dual RNA-seq uncovers metabolic amino acids dependency of the intracellular bacterium *Piscirickettsia salmonis* infecting Atlantic salmon. Front. Microbiol. 9, 11. https://doi.org/10.3389/fmicb.2018.02877.

Wei, D., Cheng, Y., Xiao, S., Liao, W., Yu, Q., Han, S., Huang, S., Shi, J., Xie, Z., Li, P., 2023a. Natural occurrences and characterization of *Elizabethkingia miricola* infection in cultured bullfrogs (*Rana catesbeiana*). Front. Cell. Infect. Microbiol. 13, 1094050. https://doi.org/10.3389/fcimb.2023.1094050/full.

Wei, D.D., Cheng, Y., Xiao, S.Y., Liao, W.Y., Yu, Q., Han, S.Y., Huang, S.S., Shi, J.G., Xie, Z.S., Li, P.F., 2023b. Natural occurrences and characterization of *Elizabethkingia miricola* infection in cultured bullfrogs (*Rana catesbeiana*). Front. Cell. Infect. Microbiol. 13, 11. https://doi.org/10.3389/fcimb.2023.1094050.

Wei, Y., Zhang, H., Gao, Z.Q., Wang, W.J., Shtykova, E.V., Xu, J.H., Liu, Q.S., Dong, Y.H., 2012. Crystal and solution structures of methyltransferase RsmH provide basis for methylation of C1402 in 16S rRNA. J. Struct. Biol. 179 (1), 29–40. https://doi.org/10.1016/j.jsb.2012.04.011.

Wu, C., Zhang, J., Zhu, G., Yao, R., Chen, X., Liu, L., 2019. *Cg* Hog1-mediated *Cg* Rds2 phosphorylation alters glycerophospholipid composition to coordinate osmotic stress in *Candida glabrata*. Appl. Environ. Microb. 85 (6). https://doi.org/10.1128/AEM.02822-18 e02822-02818.

Xia, Z.C., Zhou, X.L., Li, J.Y., Li, L., Ma, Y., Wu, Y., Huang, Z., Li, X.R., Xu, P.X., Xue, M., 2019. Multiple-omics techniques reveal the role of glycerophospholipid metabolic pathway in the response of *Saccharomyces cerevisiae* against hypoxic stress. Front. Microbiol. 10, 12. https://doi.org/10.3389/fmicb.2019.01398.

Xiao, W., Gao, Z., Liu, T., Zhong, W., Jiang, S., He, M., Fu, F., Li, G., Su, D., Guo, J., 2024a. Lemon essential oil nanoemulsions: potential natural inhibitors against *Escherichia coli*. Food Microbiol. 119, 104459. https://doi.org/10.1016/j.fm.2023.104459.

Xiao, W.B., Gao, Z.P., Liu, T., Zhong, W.M., Jiang, S.F., He, M.W., Fu, F.H., Li, G.Y., Su, D. L., Guo, J.J., Shan, Y., 2024b. Lemon essential oil nanoemulsions: potential natural inhibitors against *Escherichia coli*. Food Microbiol. 119, 11. https://doi.org/10.1016/j.fm.2023.104459.

Xie, Z.Y., Zhou, Y.C., Wang, S.F., Mei, B., Xu, X.D., Wen, W.Y., Feng, Y.Q., 2009. First isolation and identification of *Elizabethkingia meningoseptica* from cultured tiger frog, *Rana tigerina rugulosa*. Vet. Microbiol. 138 (1–2), 140–144. https://doi.org/10.1016/j.vetmic.2009.02.011.

Yang, C., Liu, Z., Yu, S., Ye, K., Li, X., Shen, D.X., 2021. Comparison of three species of *Elizabethkingia* genus by whole-genome sequence analysis. FEMS Microbiol. Lett. 368 (5), 10. https://doi.org/10.1093/femsle/fnab018.

Yang, S., Si, C., Mani, R., Keller, J., Hoenerhoff, M.J., 2023. Septicemia caused by an emerging pathogen, *Elizabethkingia miricola*, in a laboratory colony of African dwarf frogs (*Hymenochirus curtipes*). Vet. Pathol. 60 (3), 394–401. https://doi.org/10.1177/03009858231155415.

Zhang, M.M., Yan, Q.P., Mao, L.L., Wang, S.Y., Huang, L.X., Xu, X.J., Qin, Y.X., 2018. *KatG* plays an important role in *Aeromonas hydrophila* survival in fish macrophages and escape for further infection. Gene 672, 156–164. https://doi.org/10.1016/j.gene.2018.06.029.

Zhao, Y.Q., Cheng, X.L., Wang, G.H., Liao, Y., Qing, C., 2020. Linalool inhibits 22Rv1 prostate cancer cell proliferation and induces apoptosis. Oncol. Lett. 20 (6), 8. https://doi.org/10.3892/ol.2020.12152.

Zhou, P., Yuan, X.K., Liu, H., Qi, Y.L., Chen, X.L., Liu, L.M., 2020. *Candida glabrata* Yap6 recruits Med2 to alter glycerophospholipid composition and develop acid pH stress resistance. Appl. Environ. Microb. 86 (24), 20. https://doi.org/10.1128/aem.01915-20.